Research Article | Vol. 27, No. 14 / 8 July 2019 / Optics Express 19906

Optics EXPRESS

Independent dual single-sideband vector millimeter-wave signal generation by one single I/Q modulator

XIAOLONG PAN,[1,2,*] XIANGYU LIU,[1,2] HONGXIN ZHANG,[1,2] KAIHUI WANG,[3] YUEMIN ZHANG,[1,2] DONGSHENG RAN,[1,2] XISHUO WANG,[1,2] AND CHUXUAN WANG[1,2]

[1] *School of Electronic Engineering, Beijing University of Posts and Telecommunications (BUPT), Xitucheng Road NO. 10, Beijing, 100876, China*

[2] *Key Laboratory of Space-ground Interconnection and Convergence, Beijing University of Posts and Telecommunications (BUPT), Xitucheng Road NO. 10, Beijing, 100876, China*

[3] *Laboratory for Information Science of Electromagnetic Waves (MoE), Department of Communication Science and Engineering, Fudan University, No. 220, Handan Road, Shanghai 200433, China*

[*] *panxiaolong2018@126.com*

Abstract: We propose a new scheme to realize the independent dual single-sideband (SSB) vector millimeter-wave (mm-wave) signal generation based on one single in-phase/quadrature (I/Q) modulator. The two SSB vector mm-wave signals can have independent carrier frequencies and modulation formats. We experimentally demonstrate the simultaneous generation and transmission of 38 GHz 16-ary quadrature-amplitude-modulation (16QAM) and 40 GHz quadrature-phase-shift-keying (QPSK) mm-wave signals based on this scheme. The penalty of the 16QAM and QPSK mm-wave signals after transmission over 10-km standard single-mode fiber and 0.5-m wireless link can be neglected.

1. Introduction

The radio-over-fiber (ROF) technology can provide huge transmission bandwidth and long transmission distance for mobile data communication, which is a hot topic in recent years [1–6]. For the practical implementation of the ROF technology, it is vital to generate optical millimeter-wave (mm-wave) signals with high performance, low cost and flexible modulation formats [7–9]. By using the external modulator, we can generate double-sideband (DSB) [7,10–17], single-sideband (SSB) [7,9,18–22] and optical-carrier-suppression (OCS) [7,16] mm-wave signals. In order to realize relatively long-distance fiber transmission, the SSB modulation is a good scheme since it can overcome walk-off effects caused by fiber dispersion [7]. In [22], X. Li et al. show that we can realize optical SSB modulation based on an in-phase/quadrature (I/Q) modulator, and enabled by this scheme, the W-band optical mm-wave signals with single-carrier quadrature-phase-shift-keying (QPSK) modulation at 4Gbaud were generated. In [23], the SSB orthogonal-frequency-division-multiplexing (OFDM) mm-wave signal was generated based on a single I/Q modulator. The real wireless networks should provide multiple-frequency access to satisfy different kinds of services [24–26]. To the best of our knowledge, the current WiFi technology provides two or three different carrier frequencies, in order to provide different bandwidths and to reduce crosstalk between the neighboring WiFi cable moderns [24]. However, in the previous demonstrations, the data carried by different frequencies is identical [25,26]. However, using different frequencies to carry different data can provide more flexibility for the future ROF networks.

In this paper, we propose a new scheme to generate the dual-frequency optical mm-wave carrier simultaneously employing two different kinds of vector modulation formats, based on a

#367538 https://doi.org/10.1364/OE.27.019906
Journal © 2019 Received 16 May 2019; revised 9 Jun 2019; accepted 9 Jun 2019; published 2 Jul 2019

Optics EXPRESS

single I/Q modulator and the dual-SSB modulation. The two independent frequencies as well as the two independent vector modulation formats of the dual-frequency optical mm-wave carrier can be software defined, and therefore our scheme is very flexible.

2. Principle

Figure 1 shows our scheme to generate the two independent SSB vector mm-wave signals based on a single I/Q modulator. The driving signal S_E for the I/Q modulator, which can be generated via offline digital signal processing (DSP) [27], can be expressed as:

$$S_E = Ae^{(-i2\pi f_1 t)} + Be^{(i2\pi f_2 t)} \tag{1}$$

Here, we use $-f_1$ and f_2 to denote the sideband frequencies of the lower-sideband (LSB) and upper-sideband (USB) vector signals, respectively. Both f_1 and f_2 are positive, and they can be identical or different. We use two complex parameters, A and B, to denote the transmitter data carried by the LSB and USB vector signals, respectively. Both A and B can employ single-carrier or OFDM vector quadrature-amplitude-modulation (QAM) modulation, including QPSK, 16-ary quadrature-amplitude-modulation (16QAM), and so on. Also, A and B can employ identical or different vector QAM modulation formats.

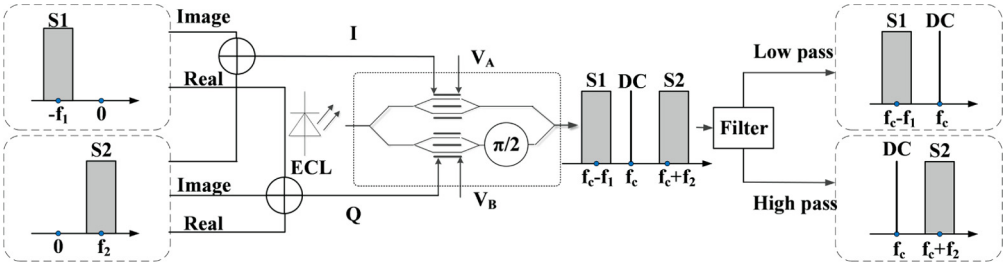

Fig. 1. The scheme of dual-SSB vector mm-wave signal generation base on a single I/Q modulator.

If A is a QPSK data, its constellation is:

$$\begin{bmatrix} -1+i & 1+i \\ -1-i & 1-i \end{bmatrix} \tag{2}$$

If B is a 16QAM data, its constellation can be described as:

$$\begin{bmatrix} -3+3i & -1+3i & 1+3i & 3+3i \\ -3+i & -1+i & 1+i & 3+i \\ -3-i & -1-i & 1-i & 3-i \\ -3-3i & -1-3i & 1-3i & 3-3i \end{bmatrix} \tag{3}$$

As shown in Fig. 1, we first add the real and imaginary parts of the LSB and USB vector signals, respectively, and then we use the real and imaginary summation to drive the I/Q modulator. If we assume the I/Q modulator follows the linear modulation, the generated optical signal from the I/Q modulator can be expressed as:

$$S_O = \alpha A e^{i2\pi(f_c - f_1)t} + \beta A e^{i2\pi(f_c + f_2)t} + \gamma e^{i2\pi f_c t} \tag{4}$$

Where α and β are the response of the I/Q modulator, and they are both constant. γ is the DC value of the optical carrier at the center wavelength after the I/Q modulator, which can be changed

Optics EXPRESS

by adjusting V_A and V_B. Here, V_A and V_B denote the DC biases of the two intensity modulators in the upper and lower arms of the I/Q modulator, respectively. f_C is the frequency of the optical carrier at the center wavelength. The schematic output spectrum of the I/Q modulator can be described by inset (b) in Fig. 1. We can adjust V_A and V_B to obtain a proper γ. After fiber transmission, we use the optical filtering to choose the optical carrier and only one sideband. As a result, we can simultaneously generate two independent optical mm-wave signals carrying different vector-modulated transmitter data at different carrier frequencies.

The schematic spectrum of the two independent optical mm-wave signals can be described by inset (c) in Fig. 1. It is worth noting that the optical carrier at the center wavelength is split into two equal parts after the optical filtering. Two optical mm-wave signals can be therefore expressed as:

$$S_{LSB} = \alpha A e^{i2\pi(f_c - f_1)t} + 1/2\gamma e^{i2\pi f_c t} \tag{5}$$

$$S_{LSB} = \beta A e^{i2\pi(f_c + f_2)t} + 1/2\gamma e^{i2\pi f_c t} \tag{6}$$

The electrical mm-wave signals, corresponding to the LSB and USB, after detected by a photodiode (PD), can be expressed as $1/2\gamma\alpha A e^{-i2\pi f_1 t}$ and $1/2\gamma\beta B e^{i2\pi f_2 t}$, respectively. By this way, we can get two independent vector mm-wave signals at different carrier frequencies (f_1 or f_2).

3. Experimental setup

Figure 2 shows the experimental setup for the generation and delivery of 16QAM mm-wave signal at 38 GHz and QPSK mm-wave signal at 40 GHz based on one I/Q modulator. We

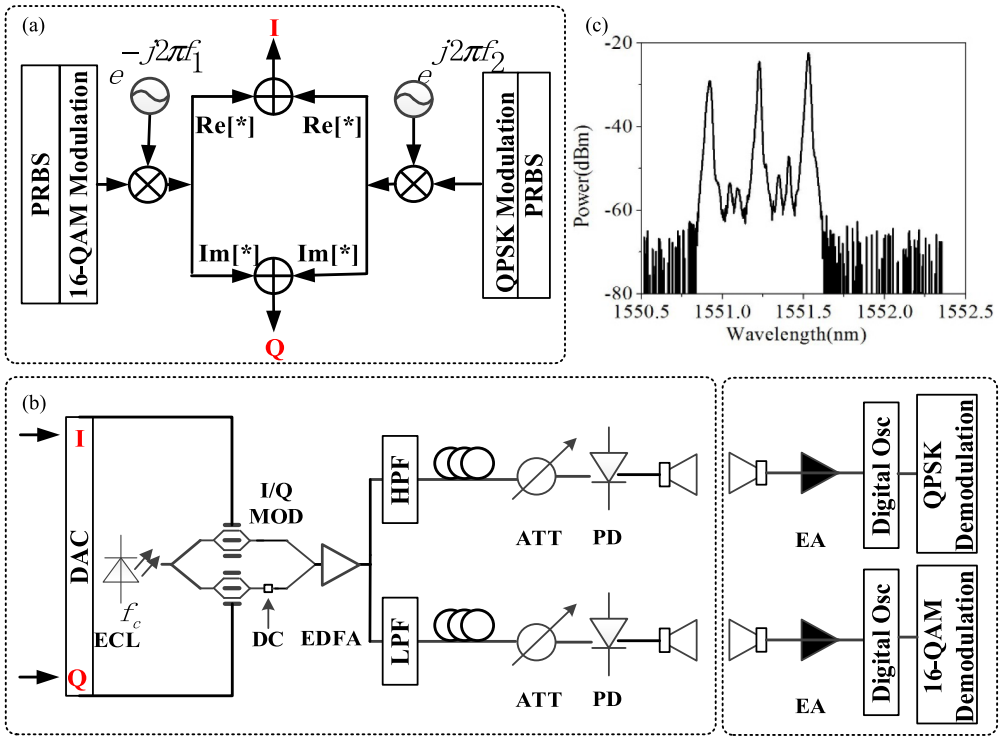

Fig. 2. Experimental setup for the generation and delivery of 16-QAM mm-wave signal at 38 GHz and QPSK mm-wave signal at 40 GHz. (a) DSP of transmission side; (b) Received Side and (c) Optical spectra after I/Q modulator.

Optics EXPRESS

simultaneously generate the 16QAM signal at 38 GHz (LSB) and QPSK signal at 40 GHz (USB), i.e., S_E described in Eq. (1), in the digital domain using MATLAB programming, before we upload it to the 92-GSa/s digital-to-analog converter (DAC) with 3-dB bandwidth of 22 GHz. Here, the pseudo-random-binary-sequence (PRBS) length of the QPSK and 16QAM signals is 2^{10} and 2^{11}, respectively. The I (the imaginary part of S_E) and Q (the real part of S_E) signals from the 92-GSa/s DAC are first simultaneously amplified and then used to drive an I/Q modulator with 30 GHz optical bandwidth. The continuous-wavelength (CW) lightwave at 1551.528 nm is generated from an external cavity laser (ECL) with < 100-kHz linewidth and 14 dBm output power, and it is used as the optical input of the I/Q modulator. The output optical power of the I/Q modulator is −10dBm. Here, the total optical power loss of 24 dB after the I/Q modulator is caused by the insertion loss and limited 30 GHz optical bandwidth of the I/Q modulator, since the 30 GHz optical bandwidth is insufficient to support the 38- and 40 GHz mm-wave frequencies. Moreover, although the output amplitude of the 92-GSa/s DAC is up to 800 mV at 10 GHz, it is only less than 100 mV at ~40 GHz. So we then use an Erbium Doped Fiber Amplifier (EDFA) to boost the optical power to be 12dBm. Figure 2(c) shows the output optical spectrum of the I/Q modulator, showing a 16QAM-moduated optical LSB and a QPSK-modulated optical USB.

We adjust the DC-bias of the I/Q modulator to ensure that the central optical carrier has a proper power which is close to that of LSB and USB. First, we adjust three DC-bias to make modulator normal work by using a QPSK signal. Figure 3 shows an IQ modulator with three DC biases. Once the QPSK is generated, it means that the DC bias on the waveguide to generate a pi/2 phase delay (PD). Then we adjust the DC_1 bias on MOD_1 to make the output power of the optical carrier is equal to that of one SSB signal (LSB in this experiment). After that, we adjust the DC_2 bias on MOD_2 to make that the output power of the optical carrier has a power larger than 3 dB of that of the one SSB signal (LSB in this experiment). Because the DC bias is shifted from the point of the minimal output power, the optical power of the central carrier become large. But the linear performance of the MOD will become worse once the DC bias is moved from this point. It will have some nonlinear effects such as unequal amplitude for higher order QAM, so the performance will be degraded a little bit.

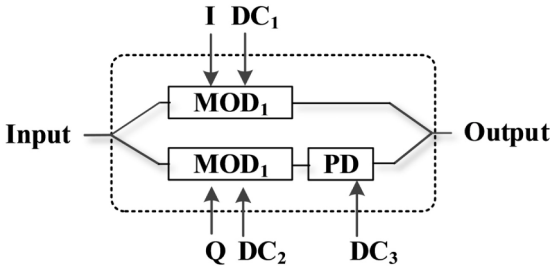

Fig. 3. The scheme of I/Q modulator.

Next, the dual-SSB optical mm-wave signal is divided into two parts by a 50/100 GHz optical interleaver. The 3 dB bandpass of the optical interleaver is 35 GHz; and the insertion loss is 1.5 dB. Figures 4(a) and 4(b) show the optical spectra of the two signals after the optical interleaver with the resolution of 0.02 nm, respectively. It is clearly seen that the 38 GHz 16QAM signal and 40 GHz QPSK signal are separated perfectly. And the two signals are input into 10-km standard single-mode fiber (SSMF) with the input power of 8dBm. After 10-km SSMF transmission without optical dispersion compensation, the signals are detected by two parallel single-ended PDs, each with 40 GHz optical bandwidth. The variable optical attenuator (VOA) before each PD is used to adjust the input power into the PD to measure the bit-error-ratio (BER). After amplified by two parallel broadband radio-frequency (RF) amplifiers, each with an operating

Optics EXPRESS

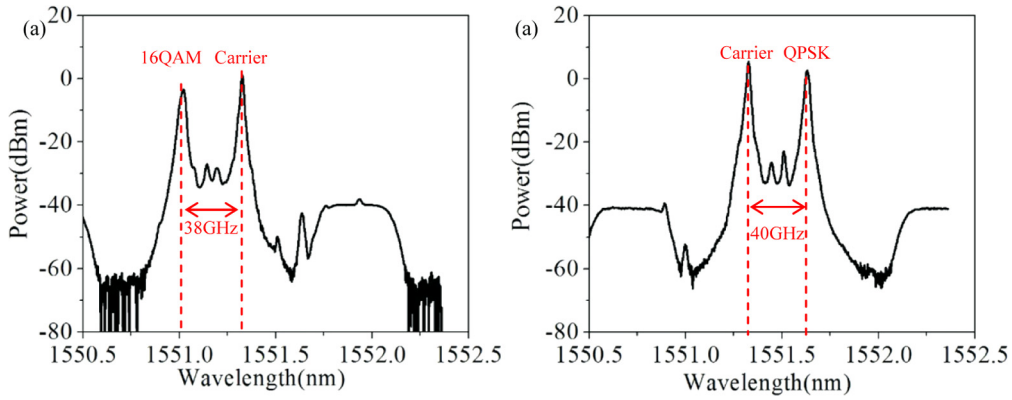

Fig. 4. Optical spectra: (a) output 16QAM signal at 38 GHz from optical interleaver; (b) output QPSK signal at 40 GHz from optical interleaver.

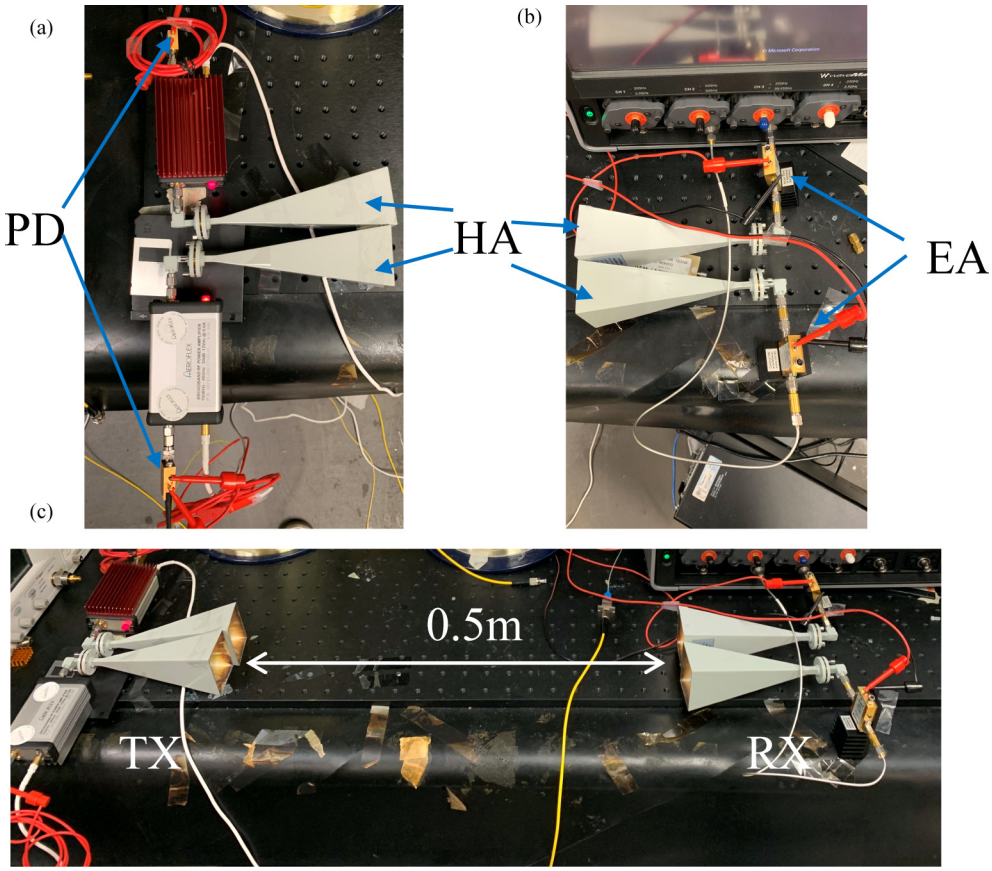

Fig. 5. The photo of wireless link. (a) Transmitter side, (b) receiver side, and (c) whole link.

frequency range from 100kHz to 40 GHz and a gain of 30 dB, the 38 and 40 GHz electrical mm-wave signals are simultaneously radiated by a pair of Q-band horn antenna (HAs) into air space, and then received by another pair of Q-band HAs. The two pairs of HAs, each with 25-dBi gain, are identical, and have a 0.5-m wireless separation. At the wireless receiver end, the

Optics EXPRESS

two signals pass through two parallel linear broadband amplifiers (90kHz - 60 GHz), and then are simultaneously captured by a 120-GSa/s real-time digital storage oscilloscope (OSC) with 45 GHz electrical bandwidth. Figures 5(a)–5(c) give the photos of the wireless transmitter end, the wireless receiver end, and the 0.5-m wireless transmission link, respectively. The received data is recovered by offline DSP with heterodyne detection [28–30], including down conversion to baseband, constant modulus algorithm (CMA) for QPSK and cascaded multi-modulus algorithm (CMMA) for 16QAM, frequency offset estimation, phase offset estimation, decision-directed least-mean-square (DD-LMS) equalization for 16QAM, and BER calculation [31–34]. Here we use CMA and CMMA to equalize the signal. Because the carrier frequency is much higher than the bandwidth of the DAC, the SSB signals are suffered from strong filter effects. Also DD-LMS equalization can further compensate the filtering effect.

4. Experimental Result

Figure 6 gives the measured BER versus the input optical power into PD for 2-Gbaud 38 GHz 16QAM and 40 GHz QPSK mm-wave signals in four different cases: (1) without fiber and wireless transmission (BtB), (2) with 0.5-m wireless transmission only (Wireless), (3) with 10-km SSMF transmission only (Wireline), and (4) with both 10-km SSMF transmission and 0.5-m wireless transmission (Wireline and Wireless). The BER of both the QPSK and 16QAM signals can be smaller than 1×10^{-5} for all the four cases. For the 16QAM signal, as shown in Fig. 6(a), when the input power is larger than −9dBm, there will be no error in the BtB case; when the input power reaches −8dBm, no error is recorded in all the other three cases; when the input power is larger than −11dBm, the BER of all the four cases can reach signal, as shown in Fig. 6(b), when the input power is larger than −7.5dBm, the BER can be smaller than 1×10^{-5} for all the four cases. Meanwhile, we can find that the −10.5-dBm input power can make BER smaller than the HD-FEC threshold for all the four cases. It is worth noting that, almost no penalty is caused by 0.5-m wireless or 10-km SSMF transmission for both the 38 GHz 16QAM signal and 40 GHz QPSK signal. Our DAC's bandwidth at 3 dB is around 22 GHz, so the response at 38~40 GHz is not good. Also the electrical amplifier to boost the signals from the DAC has 3 dB 32 GHz bandwidth. At 40 GHz, the response of the electrical amplifier is not good, but at 38 GHz it is much better. Due to the two reasons, the sensitivity of 16QAM at 38 GHz is better than that of QPSK at 40 GHz.

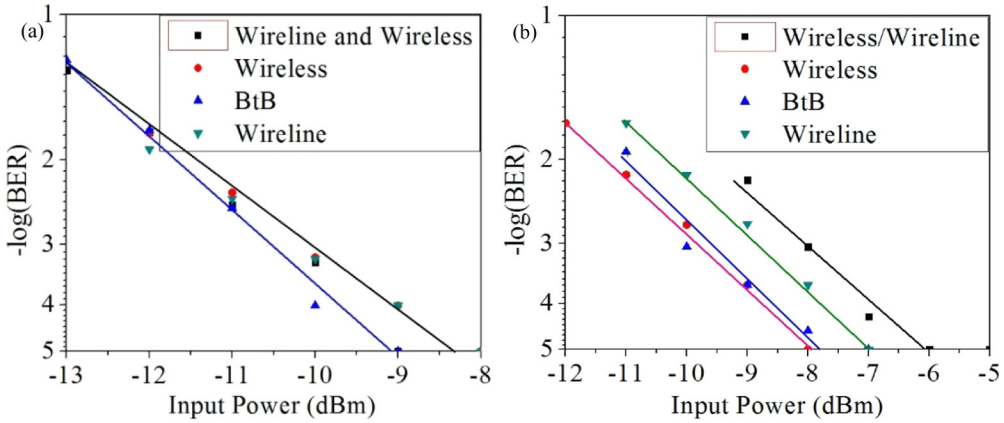

Fig. 6. Measured BER versus input power into PD for (a) 38 GHz 16QAM signal and (b) 40 GHz QPSK signal.

Figure 7 gives the received constellations of 16QAM and QPSK after 10-km SSMF and 0.5-m wireless transmission at the input power into PD of −8dBm and −7dBm, respectively.

Optics EXPRESS

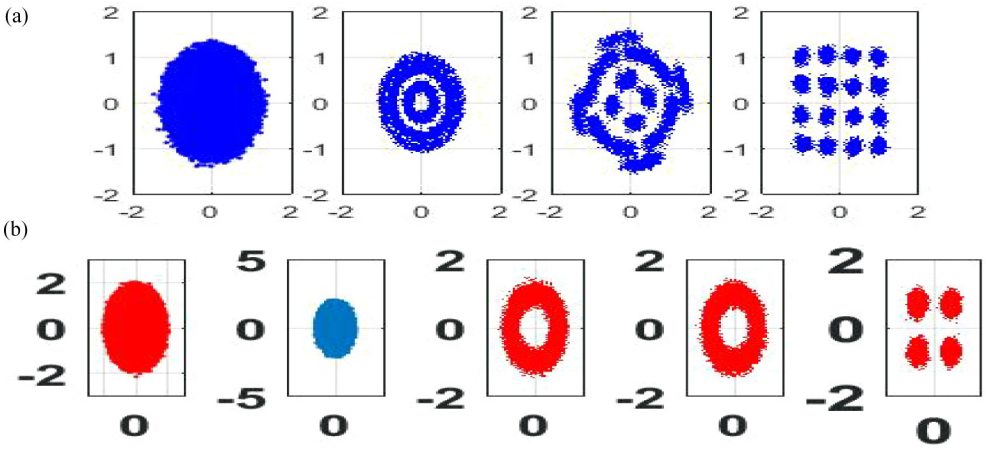

Fig. 7. (a) Constellations of 38 GHz 16QAM signal after 10-km SSMF and 0.6-m wireless transmission with an input power of −8dBm: (i) after resampling, (ii) after CMMA, (iii) after frequency offset estimation, and (iv) after phase offset estimation. (b) Constellations of 40 GHz QPSK signal after 10-km SSMF and 0.6-m wireless transmission with an input power of −7dBm: (i) before resampling, (ii) after resampling, (iii) after CMA, (iv) after frequency offset estimation, and (v) after phase offset estimation.

For both 16QAM and QPSK, no bit error is recorded within the collected data. Insets (i)-(iv) in Fig. 7(a) correspond to the DSP procedure after resampling, after CMMA, after frequency offset estimation, and after phase offset estimation, respectively. Insets (i)-(v) in Fig. 7(b) correspond to the DSP procedure before resampling, after resampling, after CMA, after frequency offset estimation, and after phase offset estimation, respectively.

We also experimentally investigated the system performance when the baudrate of the QPSK and 16QAM signals is increased to 4Gbaud. However, because of the bandwidth limitation of the 92-GSa/s DAC, the 40 GHz QPSK signal at 4Gbaud cannot be recovered in this system. The BER performance of the 38 GHz 16QAM signal is shown in Fig. 8. Compared with the 2-Gbaud case shown in Fig. 6(a), the 4-Gbaud case needs an additional 2-dBm input power into PD, that is, a total of −9dBm, to reach a BER smaller than the HD-FEC threshold.

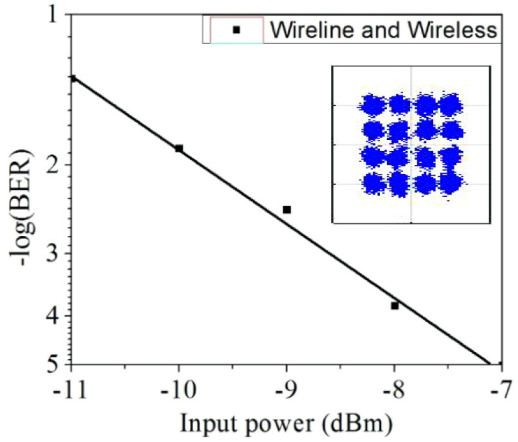

Fig. 8. BER and constellation of 4Gbaud 16QAM mm-wave signal at 38 GHz.

Optics EXPRESS

5. Conclusions

We have demonstrated how to generate two independent vector mm-wave signals at different carrier frequencies based on a single I/Q modulator. In our scheme, we generate USB and LSB optical signals by an I/Q modulator driven by our designed electrical signals. Then we use an optical interleaver with one input and two outputs to separate the USB and LSB optical signals for the generation of two independent optical mm-wave signals. Using our scheme, we experimentally demonstrate the simultaneous generation of 2-Gbaud 40 GHz QPSK and 2-Gbaud 38 GHz 16QAM mm-wave signals. We also realize the simultaneous error-free transmission of these two independent mm-wave signals over 10-km wireline and 0.5-m wireless link. Due to the bandwidth limitation of our employed DAC, we can only realize 4-Gbaud 38 GHz 16QAM mm-wave signal delivery, while 4-Gbaud 40 GHz QPSK mm-wave signal delivery has a BER larger than the FEC threshold.

Funding

National Natural Science Foundation of China (NSFC) (61527801, 61675048, 61720106015, 61805043, 61835002).

References

1. D. Zibar, R. Sambaraju, A. Caballero, J. Herrera, U. Westergren, A. Walber, J. B. Jensen, J. Martí, and I. T. Monroy, "High-capacity wireless signal generation and demodulation in 75- to 110 GHz band employing alloptical OFDM," IEEE Photonics Technol. Lett. **23**(12), 810–812 (2011).
2. X. Li, Z. Dong, J. Yu, N. Chi, Y. Shao, and G. K. Chang, "Fiber wireless transmission system of 108-Gb/s data over 80-km fiber and 2×2 MIMO wireless links at 100 GHz W-Band frequency," Opt. Lett. **37**(24), 5106–5108 (2012).
3. Z. Cao, J. Yu, M. Xia, Q. Tang, Y. Gao, W. Wang, and L. Chen, "Reduction of intersubcarrier interference and frequency-selective fading in OFDM-ROF systems," J. Lightwave Technol. **28**(16), 2423–2429 (2010).
4. C. Liu, H. C. Chien, S. H. Fan, J. Yu, and G. K. Chang, "Enhanced vector signal transmission over doublesideband carrier-suppressed optical millimeter-waves through a small LO feedthrough," IEEE Photonics Technol. Lett. **24**(3), 173–175 (2012).
5. X. Li, J. Yu, J. Zhang, Z. Dong, F. Li, and N. Chi, "A 400G optical wireless integration delivery system," Opt. Express **21**(16), 18812–18819 (2013).
6. J. Yu, X. Li, and N. Chi, "Faster than fiber: over 100-Gb/s signal delivery in fiber wireless integration system," Opt. Express **21**(19), 22885–22904 (2013).
7. J. Yu, Z. Jia, L. Yi, Y. Su, G. K. Chang, and T. Wang, "Optical millimeter-wave generation or up-conversion using external modulators," IEEE Photonics Technol. Lett. **18**(1), 265–267 (2006).
8. M. Attygalle, C. Lim, G. J. Pendock, A. Nirmalathas, and G. Edvell, "Transmission improvement in fiber wireless links using fiber Bragg gratings," IEEE Photonics Technol. Lett. **17**(1), 190–192 (2005).
9. Y. Xu, X. Li, J. Yu, and G. Chang, "Simple and reconfigured single-sideband," Opt. Express **24**(20), 22830–22835 (2016).
10. C. T. Lin, J. Chen, P. T. Shih, W. J. Jiang, and S. Chi, "Ultra-High Data-Rate 60 GHz Radio-Over-Fiber Systems Employing Optical Frequency Multiplication and OFDM Formats," J. Lightwave Technol. **28**(16), 2296–2306 (2010).
11. J. Ma, "Dual-tone QPSK optical millimeter wave signal generation by frequency-nonupling the RF signal without phase precoding," IEEE Photonics J. **8**(4), 1–7 (2016).
12. C. T. Lin, Y. M. Lin, J. Chen, S. P. Dai, P. T. Shih, P. C. Peng, and S. Chi, "28-Gb/s 16QAM OFDM radio-over-fiber system within 7 GHz license-free band at 60 GHz employing all-optical up-conversion," Opt. Express **16**(9), 6056–6063 (2008).
13. X. Chen and J. Yao, "Wavelength Reuse in an RoF Link Based on CS-DSB, Coherent Detection and DSP," IEEE Photonics Technol. Lett. **29**(12), 975–978 (2017).
14. X. Li, J. Yu, J. Zhang, J. Xiao, Z. Zhang, Y. Xu, and L. Chen, "QAM Vector Signal Generation by Optical Carrier Suppression and Precoding Techniques," IEEE Photonics Technol. Lett. **27**(18), 1977–1980 (2015).
15. W. Zhou, X. Li, and J. Yu, "Pre-coding assisted generation of a frequency quadrupled optical vector D-band millimeter wave with one Mach-Zehnder modulator," Opt. Express **25**(22), 26483–26491 (2017).
16. X. Li, J. Xiao, Y. Xu, and J. Yu, "QPSK Vector Signal Generation Based on Photonic Heterodyne Beating and Optical Carrier Suppression," IEEE Photonics J. **7**(5), 1–6 (2015).
17. A. Kanno, K. Inagaki, I. Morohashi, T. Sakamoto, T. Kuri, I. Hosako, T. Kawanishi, Y. Yoshida, and K. Kitayama, "40 Gb/s W-band (75-110 GHz) 16QAM radio-over-fiber signal generation and its wireless transmission," Opt. Express **19**(26), B56–B63 (2011).
18. G. H. Smith, D. Novak, and Z. Ahmed, "Technique for optical SSB generation to overcome dispersion penalties in fibre-radio systems," Electron. Lett. **33**(1), 74–75 (1997).

Optics EXPRESS

19. J. Ma and W. Zhou, "Joint influence of the optical carrier-to-sideband ratio and guard band on direct-detection SSB-OOFDM system," IEEE Photonics J. **7**(5), 1–13 (2015).
20. R. Deng, J. Yu, J. He, M. Chen, Y. Wei, L. Zhao, Q. Zhang, and X. Xin, "Twin-SSB-OFDM Transmission Over Heterodyne W-Band Fiber-Wireless System With Real-Time Implementable Blind Carrier Recovery," J. Lightwave Technol. **36**(23), 5562–5572 (2018).
21. J. Yu, M.-F. Huang, Z. Jia, T. Wang, and G.-K. Chang, "A novel scheme to generate single-sideband millimeterwave signals by using low-frequency local oscillator signal," IEEE Photonics Technol. Lett. **20**(7), 478–480 (2008).
22. X. Li, Y. Xu, and J. Yu, "Single-sideband W-band photonic vector millimeter-wave signal generation by one single I/Q modulator," Opt. Lett. **41**(18), 4162–4165 (2016).
23. X. Li, J. Yu, and G. K. Chang, "Frequency-quadrupling vector mm-wave signal generation by only one single drive MZM," IEEE Photonics Technol. Lett. **28**(12), 1302–1305 (2016).
24. "Part11: Wireless LAN Medium Access Control (MAC) and Physical Layer (PHY) Specifications: High Speed Physical Layer in the GHz Band," IEEE Std. 802.11a/D7.0, (1999).
25. Z. Jia, J. Yu, Y. Hsueh, A. Chowdhury, H. Chien, J. Buck, and G. Chang, "Multiband signal generation and dispersion-tolerant transmission based on photonic frequency tripling technology for 60 GHz radio-over-fiber system," IEEE Photonics Technol. Lett. **20**(17), 1470–1472 (2008).
26. Y. Zhang, B. Liu, and S. Ji, "Generation of Multiple-Frequency Optical Millimeter-Wave Signal With Optical Carrier Suppression and No Optical Filter," IEEE Photonics J. **9**(1), 1–7 (2017).
27. H.-C. Chien, Z. Jia, J. Zhang, Z. Dong, and J. Yu, "Optical independent-sideband modulation for bandwidth-economic coherent transmission," Opt. Express **22**(8), 9465–9470 (2014).
28. X. Li, J. Yu, J. Xiao, and Y. Xu, "Fiber-wireless-fiber link for 128-Gb/s PDM-16QAM signal transmission at Wband," IEEE Photonics Technol. Lett. **26**(19), 1948–1951 (2014).
29. L. Zhao, J. Yu, L. Chen, P. Min, J. Li, and R. Wang, "16QAM vector mm-wave signal generation based on phase modulator with photonic frequency doubling and pre-coding," IEEE Photonics J. **8**(2), 1–8 (2016).
30. J. Zhang, Z. Dong, J. Yu, N. Chi, L. Tao, X. Li, and Y. Shao, "Simplified coherent receiver with heterodyne detection of eight-channel 50 Gb/s PDM-QPSK WDM signal after 1040 km SMF-28 transmission," Opt. Lett. **37**(19), 4050–4052 (2012).
31. J. Yu and X. Zhou, "Ultra-high-capacity DWDM transmission system for 100G and beyond," IEEE Commun. Mag. **48**(3), S56–S64 (2010).
32. J. Yu, X. Li, and W. Zhou, "Tutorial: Broadband fiber-wireless integration for 5G+ communication," APL Photonics **3**(11), 111101 (2018).
33. J. Yu, "Photonics-Assisted Millimeter-Wave Wireless Communication," IEEE J. Quantum Electron. **53**(6), 1–17 (2017).
34. X. Li, J. Xiao, and J. Yu, "Long-Distance Wireless mm-Wave Signal Delivery at W-Band," J. Lightwave Technol. **34**(2), 661–668 (2016).